Materials Science in Semiconductor Processing 169 (2024) 107902

Contents lists available at ScienceDirect

Materials Science in Semiconductor Processing

journal homepage: www.elsevier.com/locate/mssp

Effect of process parameters on co-sputtered $Al_{(1-x)}Sc_xN$ layer's properties: Morphology, crystal structure, strain, band gap, and piezoelectricity

Nguyen Quoc Khánh [a,*], Zsolt Endre Horváth [a], Zsolt Zolnai [a], Péter Petrik [a,b], László Pósa [a], János Volk [a]

[a] Centre for Energy Research, Institute of Technical Physics and Materials Science, Konkoly-Thege M. út 29-33, H-1121, Budapest, Hungary
[b] Department of Electrical and Electronic Engineering, Institute of Physics, Faculty of Science and Technology, University of Debrecen, 4032, Debrecen, Hungary

ARTICLE INFO

Keywords:
$Al_{(1-x)}Sc_xN$ thin film
Pulse DC reactive ion co-sputtering
In-plane residual stress
Optical band gap
Direct and converse piezoelectricity
Piezoresponse force microscopy
X ray Diffractometry

ABSTRACT

The effect of pulse direct current (DC) reactive ion co-sputtering parameters on the morphology, crystal structure, residual stress, band gap, and piezoelectric properties of the $Al_{(1-x)}Sc_xN$ thin film deposited in large target-to-substrate distance (TSD) system has been studied using Scanning Probe Microscopy, X ray Diffractometry, Spectroscopic Ellipsometry, and profilometer, among others. The process pressure was revealed to be the key factor which essentially determines the quality of the film for such system. As low as 0.2 Pa working pressure is needed to achieve smooth nitride layer with good piezoelectric properties. High $N_2/(Ar + N_2)$ gas ratio also was shown to result in better film properties. Residual stress in nitride film, and thereby the optical band gap can be tuned by variation of process pressure, gas ratio, and Sc fraction in the studied x range (0–0.5). The $Al_{(1-x)}Sc_xN$ film deposited at low pressure, medium N_2 gas ratio with $x \sim 0.41$ shows high piezoelectric coefficient, relatively low residual stress, and smooth surface. Top electrode has been applied to eliminate the interfering effect of the restraining force induced by the unexcited matrix materials around tip/sample contact for Piezoresponse Force Microscopic (PFM) measurement of piezoelectric constant of thin nitride film. We have shown by comparing the corrected d_{33corr} data determined with PFM to those obtained from direct piezoelectric method that PFM using proper measurement conditions and correction can be applied as a quantitative method for study of piezoelectric properties of thin film.

1. Introduction

Wide bandgap piezoelectric AlN is a potential candidate as active material for sensors [1–3], energy harvesters [4–6] and telecommunication [7,8] owing to its outstanding properties, such as piezoelectricity even at high temperature, extreme hardness, good thermal and chemical stabilities, biocompatibility, compatibility to MEMS technology, and not least, environment friendly lead-free material [9,10]. It has been shown that AlN moderate piezoelectric constant, d_{33} could be improved by alloying AlN with ScN [11] or YN [12]. Introducing Sc to AlN, however, can also modify its bandgap [13] which open the possibility of fully integrated III-N piezo-, optoelectronics systems for the aforementioned applications.

To this end, reactive co-sputtering of Al and Sc targets is the most flexible technique with reasonable output, because nitride thin film with various metal compositional ratio can be easily achieved [11,14,15]. In co-sputtering deposition system, there is the need of having long target to substrate distance (TSD) to make room for targets, and to enable small target tilting angle, for which the sputtered particles moving toward the substrate is highly oriented in the paraxial directions. Film deposition under this condition suffers less self-shadowing [16], i.e. it is dense and can be free of void.

Generally, growth of high quality crystalline nitride layer in *c*-direction is demanded, because it gives the best piezoelectric response. The key process for desired growth is to prevent the formation of metal-N dimers in plasma via scattering of sputtered particles on ions [17,18], which promotes crystal growth in other directions than *c*-axis. High kinetic energy of the arriving particles is also necessary to ensure high surface diffusion of adatoms for good crystal growth. From this point of view, low working pressure is preferred, because it means large free path length, thus reduces the scattering of sputtered particles on plasma ions, i.e. less energy loss of the sputtered particles [17,19]. The N_2 gas ratio, i.e. $N_2/(Ar + N_2)$ was reported to slightly affect the dominating 002 oriented crystalline quality, but has significant impact on the formation

* Corresponding author. EK MFA, 1525, Budapest, P.O. Box 49. Hungary.
E-mail address: n.q.khanh@ek.hun-ren.hu (N.Q. Khánh).

https://doi.org/10.1016/j.mssp.2023.107902
Received 4 September 2023; Received in revised form 8 October 2023; Accepted 9 October 2023
Available online 14 October 2023

of the so-called abnormal oriented grains (AOGs) of deposited nitride film [20]. High N_2 gas ratio is energetically favorable for crystal growth along *c*-axis, while low ratio promotes growth in *a*, or other directions [21].

Though low working pressure or/and high N_2 gas ratio are beneficial for preferential growth direction in c-axis, they may cause high compression stress via peening effect, which is the most typical stress enhancing mechanism for layer deposition by sputtering [19,22]. The residual stress has been shown as a crucial issue in device operation [23]. Nevertheless, there are few works studying the residual stress in AlScN film deposited by co-sputtering. For example, Fichtner et al. showed deposition parameters like pressure, gas ratio, and power fraction of targets can affect stress formation [24]. However, few presented data, and also the overlap of varying parameters do not make it easy to show the clear correlation between the parameters and stress. Dependence of film properties, like crystal structure and piezoelectricity on Sc content has been well investigated so far [11,15,25,26], but less studied in terms of stress, where crystal lattice softening with increasing Sc content [27,28] may influence the formation of the in-plane stress in AlScN film.

In study of the piezoelectric properties of thin films, direct piezoelectric method (Berlincourt type piezometer) [29] is frequently applied, which measures the average value of d_{33}. For mapping piezoelectric constant in nano scale, converse piezoelectricity based Piezoresponse Force Microscopy (PFM) [30], could be an appropriate technique, where the electromechanical (EM) displacement generated by electric field is measured. However, the displacement measured by PFM is not only originated from pure piezoelectric effect, but it also contains the contribution of other interfering effects, like electrostatic force [31], electrostriction [32], flexoelectricity [33], electrochemical strain [34], which make the quantification of PFM measurement difficult.

The contribution of the electrostatic force as dominant non-piezoelectric impact can be eliminated by using a stiff cantilever [35,36]. In PFM measurement, a sharp conductive AFM tip is used to drive the excitation V_{ac} voltage. Therefore, the restraining force of the unexcited matrix materials around the tip/sample contact area against the EM displacement is strong, because it is proportional to the ratio of contact perimeter and excited area under tip. Decreasing the restraining force may result in more reliable the measured data [37]. Furthermore, the bottom of the film is also clamped by the inactive substrate, which restrains the volume change of the film along the substrate surface. This so called clamping effect of substrate should be taken into accounts for correct result of PFM [38].

In this article we report on the effect of deposition parameters, i.e. gas pressure and composition, as well as input power ratio on the comprehensive properties of pulse DC magnetron co-sputtered thin $Al_{(1-x)}Sc_xN$ films, and on the PFM study of their piezoelectricity. Top electrodes and substrate effect corrections were applied for achieving reliable quantified results, based on which a simple formula was proposed to determine the distribution of d_{33} in nanoscale. All show the applicability of PFM as a quantitative method for the study of the piezoelectric properties of thin films.

2. Experimental

2.1. Sample preparation

3" <100> *p*-Si wafers with thickness of 380 μm have been used as substrates for nitride deposition. They were ultrasonically cleaned stepwise in acetone, ethanol, deionized water for 5 min, and purged in nitrogen. Then the wafer was loaded into the chamber of the pulse DC magnetron sputtering system (VAKSIS- MiDAS). The base pressure was in the range of 0.8–1.1 10^{-5} Pa. The substrate was further cleaned by 50 W Ar plasma for 5 min. Then $Al_{(1-x)}Sc_xN$ films were deposited onto Si substrates by reactive sputtering with a varying parameter (working pressure, gas ratio, and input power ratio) for 1 h. The sputtering cathodes were 3" pure Al (5 N) and Sc (3.5 N) targets which were continuously water cooled. The Al target was set face to face with the substrate, while the Sc one was tilted by ca. 27° to the substrate normal. Both of them were set eccentrically to the rotating substrate ensuring the film thickness uniformity. The gases used are high-purity argon (5 N) as working gas, and nitrogen (5 N) as reactive gas. A throttle valve between vacuum pump and main chamber has been used to automatically keep the set gas pressure. Pulsed DC power with a 120 kHz frequency and 30 % duty cycle was applied to both targets with proper input power ratio of Al and Sc to produce nitride layer with desired Sc content. During deposition no intentional heating was applied, the estimated substrate temperature due to plasma heating is less than 100 °C. For deposition, the substrate was rotated at 10 revolutions per minute (rpm) to ensure film uniformity. The detailed deposition conditions are listed in Table 1.

2.2. Sample characterizations

Atomic Force Microscopy (AIST NT smart-SPM1000) was used to study the morphology of the $Al_{(1-x)}Sc_xN$ films in semi contact mode, as well as their piezoelectric properties in top-PFM mode. In the later one, the probe movement between scan raster points is performed in semi-contact mode, while PFM measurement is carried out in the raster points using contact mode technique. This hybrid operation mode enables the use of stiff cantilever for PFM scan, but takes longer time for a scan. Conductive probe with nominal spring constant of 42 Nm^{-1} (PPP–NCHPt, Nanosensors) was used in PFM measurement. The pressing force to the tip was kept at 60 nN for contact mode. The amplitude and frequency of the exciting V_{ac} were in the range up to 4 V and 51 kHz, respectively. The measured data have been evaluated by Gwyddion software package [39]. The average effective displacements (d_f) were determined from displacement maps containing 64 × 64 data array for each exciting V_{ac}, which then were used for linear fitting to obtain effective piezoelectric coefficient d_{33f} (Fig. S1 in supplementary information, SI). For comparison, the samples were also measured by Berlincourt piezometer (Piezotest PM300) using 10 N static force (preload), and 0.25 N dynamic force at 110 Hz frequency.

Top electrodes consisting of 5 nm Ti/30 nm Pd in 2 μm diameter were prepared on nitride film using e-lithography, e-beam vapor metal deposition, and lift-off for PFM study. Much larger, 3 mm diameter, 100 nm thick Ti top electrodes were deposited through a shadow mask for Piezometer measurements. Before metal depositions, 50 W radio frequency (RF) Ar plasma cleaning was applied for 3 min in all cases, which as we checked, induces no noticeable change in piezoelectricity. PFM and Piezometer measurements were carried out on both top electrode, and bare nitride nearby.

To investigate the crystal structure of the obtained films, a Bruker AXS D8 Discover diffractometer was used in parallel beam geometry (θ–2θ) at room temperature with Cu Kα radiation. The XRD diffractograms were obtained at scanned angle of 2θ varying from 30° to 70°. Rocking curves (ω scan) were also recorded at the 002 peak. The ellipsometric measurements were conducted at 60, 65, 70 angle of incidence, and in photon energy range from 2 to 5 eV using a Woollam M-2000DI

Table 1
Co-sputtering conditions for deposition of $Al_{(1-x)}Sc_xN$ films.

Parameters	Al	Sc
Target	Al (3″, 5 N)	Sc (3″, 3.5 N)
Target-substrate distance	14.5 cm	15 cm, 27° off normal
Sputtering power	200–450 W	200–400 W
Base pressure		0.8–1.1 10^{-5} Pa
$N_2/(Ar + N_2)$ gas ratio		30–100 %
Working gas pressure		0.2–0.53 Pa
Deposition time		1 h
Substrate temperature		<100 °C

rotating compensator instrument. The optical band gap was taken as the absorption onset ($k > 0$), which was determined by the fitting procedure of the measured data using Tauc – Lorentz model (see Fig. S2 in SI). The SEM measurements were performed by a LEO 1540XB field emission scanning electron microscope equipped with an Oxford UltimMax 40 energy dispersive X-ray spectrometer (EDS). An acceleration voltage of 10 kV was applied for EDS. For element analysis, Rutherford Backscattering Spectroscopy (RBS) was performed with 2 MeV $^4He^+$ analyzing ion beam, and the backscattered particles were detected by an ORTEC solid state detector placed at scattering angle of 165°. The average in-plane residual film stress was determined from wafer curvature measurements using a DEKTAK-XT profilometer performed pre- and post-growth of the nitride film. The stress in the film was calculated using the modified Stoney's equation for sample curvature measurement [40].

3. Results and discussion

The composition of the $Al_{(1-x)}Sc_xN$ film was determined by RBS analysis (Fig. S3 in SI). EDS was also carried out for comparison, but due to the overlap of Sc Lα peak with N Kα peak the determination of N content is not accurate. As shown by Fig. S4 in SI, the desired Sc fraction, i.e. the Sc to metal cation fraction can be achieved using proper input power ratio of Sc and Al targets.

3.1. Effect of deposition pressure and gas composition on nitride film properties

The effect of deposition parameters on the properties of the nitride films has been investigated using the samples deposited with varying parameters (working pressure, gas composition), and 263 W Al to 300 W Sc input power ratio (corresponding to $x\sim$ 0.31 in $Al_{(1-x)}Sc_xN$) for 1 h (see Table S1 in SI).

Fig. 1 shows the XRD θ-2θ diffractograms of the samples prepared at varied pressure, and different nitrogen gas ratio. Some scans were collected for longer time to improve statistics. The dominating peak at about 36° for all samples can be identified as (002) reflection of wurtzite nitride. It reveals that all the thin films have wurtzite crystal structure, and 002 is the preferential growth orientation independently on N_2 ratio and working pressure in the applied range, even at TSD of ca. 15 cm. The large full width at half of maximum of the 002 peak (see later) however, indicates that the films grow in form of 002 texture. Besides the 002 peak, other small peaks are also observable for films deposited at high pressure, or low N_2 ratio. The peaks near 32, 36.5, and 48.5° can be associated to (100), (101), and (102) reflections of wurtzite nitride, respectively. The peak around 34° is clearly seen at low pressure and high N_2 ratio cases, and might be identified as (111) reflection of cubic ScN, though it was reported to form at very high Sc content [15,26]. Therefore, further work is needed to unveil its origin. One can also observe the shift of 002 peaks and other ones to lower angle with decreasing pressure (Fig. 1a), or with increasing N_2 ratio (Fig. 1b). The Sc fractions of these samples are almost the same (ca. 0.31), therefore, the reason of the move of 002 peaks may be the compression stress formed in the thin layer during the deposition process. Fig. 2 presents the development of residual film stress as a function of working pressure (Fig. 2a), and N_2 gas ratio (Fig. 2b). More than 1.5 GPa developing compression stress results in ca. 1.2 % and 1.4 % increase of c lattice constant with pressure changing from 0.4 Pa to 0.2 Pa, or N_2 ratio changing from 30 % to 100 %, respectively. The origin of the stress has been shown to be the peening effect, i.e. the bombardment of the film surface by particles [22]. The formation of the compressive stress *vs.* gas pressure or composition seems to be strong for long TSD, probably due to the suppression of the self-shadowing effect [16]. When the working pressure decreases, the probability of the scattering of the sputtered particles on the gas molecules decreases, i.e. they arrive at film surface with higher energy, thus the peening effect is enhanced. Similar effect takes place, when the ratio of smaller cross-section of N_2 compared to Ar's increases. Higher N_2 gas ratio also means more reflected particles, i.e. nitrogen from the targets, which enhances the film surface bombardment. On the other hand, less scattering on gas molecules means less nitride dimer formation between target and substrate, and higher kinetic energy of arriving particles gives rise to high surface diffusion of the particles, all resulting in better crystal growth in 002 preferential direction as shown in Fig. 1 [17,19].

In Fig. 2, the optical band gaps determined by ellipsometry are also presented. The gap narrowing follows well the stress development for varying pressure (Fig. 2a), but only the tendency prevails for different N_2 gas ratio (Fig. 2b). Nevertheless, it is clear that stress induced by film deposition parameters, like gas pressure and composition can be used for band gap tuning. Also, the increasing of the pressure leads to a switch from compressive to tensile stress (Fig. 2a), which may be explained by the co-effect of particle penning, and O incorporation. The O content measured by EDS is around 2 at% for all compared sample. Having smaller atomic size than N, O incorporation may induce tensile stress, thus shifts the film strain to tensile stress at high pressure where the penning effect weakens.

Figs. 3 and 4 present the surface height images measured by AFM (a-d) together with 4 V V_{ac} induced EM displacement images measured by PFM (e-f) on bare surface of the layers deposited at varying working pressures, and N_2 gas ratios, respectively.

At low pressure the film surface is smooth (1.7 nm RMS), and contains some grains with 3–5 nm height. They are known as abnormally oriented grains (AOGs) [41], which have different crystal orientation along the surface normal, than 002 as revealed in Fig. 1. As the gas pressure increases, the density and the height of such grains increases, and they cover all the surface when deposition pressure reaches 0.38 Pa. For film deposited at 0.2 Pa the EM displacement map is relatively homogeneous, and shows a value of around 20 pm (Fig. 3e). One can see that, AOGs being grown in non-002 direction induce low EM

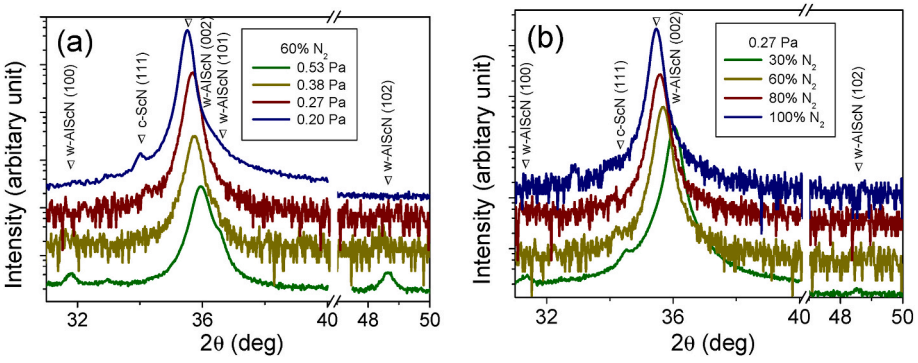

Fig. 1. XRD 2θ diffractograms of $Al_{0.69}Sc_{0.31}N$ films deposited at different working pressures with N_2 gas ratio of 60 % (a), and different N_2 gas ratios at 0.27 Pa (b). Target powers of 263 W (Al)/350 W (Sc) were applied for both cases.

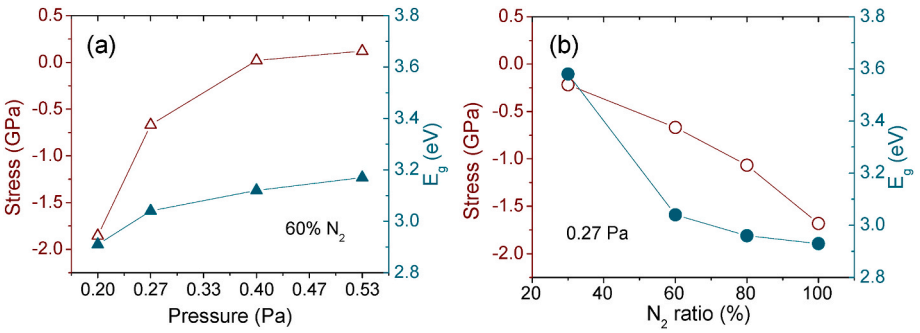

Fig. 2. In-plane residual stress (open symbol) and optical band gap (solid symbol) as a function of working pressure with 60 % N_2 gas ratio (a), and N_2 gas ratio at 0.27 Pa working pressure (b).

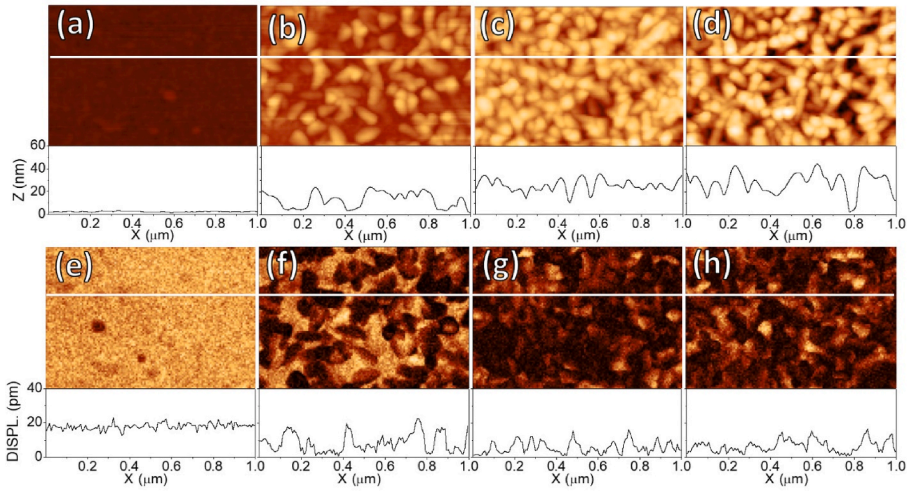

Fig. 3. Morphology and EM displacement maps of nitride film deposited at 0.2 (a,e), 0.27 (b,f), 0.38 (c,g), and 0.53 Pa (d,h) gas pressure using 263 W (Al)/350W (Sc) target powers, and N_2 gas ratio of 60 %. White lines indicate the line-cuts.

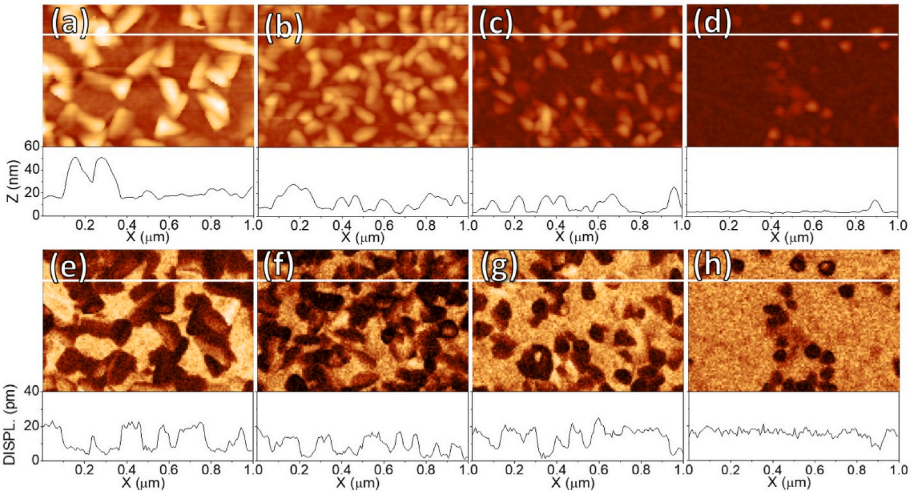

Fig. 4. Morphology and EM displacement maps of nitride film deposited using 30 % (a, e), 60 % (b, f), 80 % (c, g) and 100 % N_2 gas ratio (d, h) at 0.27 Pa with 263 W Al/350W Sc target powers. White lines indicate the line-cuts.

displacement. Higher working pressure results in less 002 oriented area, i. e. less EM displacement (Fig. 3e–h). The average displacement (d_f) calculated from the whole EM displacement map, therefore, decreases with increasing gas pressure. Similar tendency can be observed with decreasing N_2 gas ratio (Fig. 4). Using 100 % N_2 gas ratio, most area of sample surface show fine grain structure. AOGs in low density are also found, for which the EM displacement is low. As the N_2 gas ratio decreases, AOG density increases. For the case of 30 % gas ratio, the average size and height of AOG become larger, specifically 100 nm and 30 nm, respectively. The formation of AOG is consistent with the finding

reported by Supruangnet et al. [21] that nitride thin films exhibit a preferred orientation along the *a*-axis and the *c*-axis at low and high N_2 ratio of ambient gas, respectively, because the surface formation energy is lower for *a*-axis at low N_2 ratio, and for *c*-axis at high N_2 ratio.

Fig. 5 summarizes the result obtained by SPM, and XRD ω scan (Rocking curves). The areal fraction of AOGs and the surface roughness change in the similar way with pressure (Fig. 5a). At low pressure the total area of AOGs is small compared to that of fine grain region. As the pressure increases, AOG area spreads fast, so dominating the surface roughness, and it covers the whole surface at pressure higher than 0.38 Pa. This may be the consequence of the formation of metal-N dimers in plasma at present *scenario*, i.e. long TSD, high pressure, which promotes the growth in other directions than 002 [17,18] (see Fig. 1).There is the clear relationship between the effective coefficient (d_{33f}) and the full width at half of maximum (FWHM) of the rocking curves of (002) peaks, the better crystal quality, i.e. lower FWHM, the larger d_{33f} can be measured (Fig. 5b). Based on Fig. 5a, and b, 0.2 Pa seems to be the critical pressure for the co-sputtering system applying TSDs around 15 cm.

As for N_2 gas ratio dependence, AOG areal ratio just changes slightly with N_2 ratio up to 80 % (Fig. 5c). For the case of 30 % N_2 the height of large grains is larger compared to other cases, which cause the "jump" in RMS, in spite of the moderate AOG areal ratio. Using 100 % N_2, AOG ratio decreases to few percent. The N_2 gas ratios have small effect on film crystal quality as revealed by FWHM (Fig. 5d) similarly to that observed by Lu et al. [20], but the FWHM is higher in the present work probably due to lower substrate temperature, and higher Sc content. The effective coefficients measured by PFM on bare nitride show small change (within 14 %) with increasing N_2 content. In sum, combination of working pressure as low as 0.2 Pa with high N_2 gas ratio higher than 80 % may help to eliminate the formation of AOG, and improve film piezoelectric properties in our long TSD sputtering system. The residual stress controlled by process pressure and N_2 ratio may open a possibility of band gap adjusting for given Sc fraction.

3.2. Effect of target power ratio (Sc content) on nitride film properties

The Sc to cations fraction in nitride film, as shown by Fig. S3 in SI, can be tuned *via* the input power ratio applied to the targets.

Fig. 6 shows the θ-2θ scans on the nitride films having different Sc content. Similarly to the case studied in former section, the 002 remains the dominating texture in the nitride film up to at least $x = 0.41$ Sc fraction. Besides, there is a very wide peak at ca. 40°, which starts growing as the content of Sc increases. This peak is attributed to extra fine crystallite structure of cubic phase of $Al_{(1-x)}Sc_xN$. One can observe that at low Sc concentration region, the 002 peak shifts to the lower

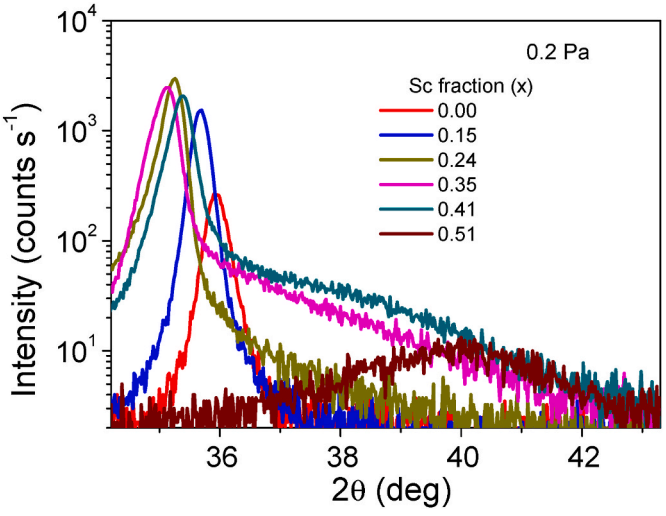

Fig. 6. XRD 2θ diffractograms of nitride films containing different Sc fraction deposited at 0.2 Pa with 60 % N_2 gas ratio.

angle with increasing Sc content. However, when the Sc fraction reaches a value as high as 0.35, this peak moves back to higher angle, while the wide peak becomes more significant. Finally, it disappears leaving only the wide peak for $x = 0.51$. The peak move in our study seems to be opposite to that reported by Satoh [15], where 002 peak moves to higher angle as the Sc fraction gets up to 0.38, then the peak move back with further Sc increase. The different behavior may originates from the fact that their studied films were rather thin (90–200 nm), and the deposition temperature was high (400 °C). Solonenko et al. showed the move of this peak to lower angle with increasing Sc fraction up to 0.35 for film deposited at 350 °C [26]. Unfortunately, no result on residual stress has been reported in these works, which also may cause the change in lattice constants, i.e. the move of diffraction peaks.

The shift of the 002 peak to lower angle with increasing Sc fraction at low concentration may be the consequence of the compression stress formation in the layer by enhanced penning effect since more arriving Sc atoms impact the film surface, together with the lattice distortion due to more incorporation of Sc having larger atomic radius than Al into Al lattice sites [25,26]. At high Sc fraction, the crystal structure is prone more and more to have cubic $Al_{(1-x)}Sc_xN$ stable phase [11,15,26]. The formation of cubic $Al_{(1-x)}Sc_xN$ nano crystallites, i.e. the wide peak in Fig. 6 seems to start at Sc fraction as low as 0.24, probably in form of two-phase mixture with wurtzite nitride, and becomes dominant for Sc fraction equal or higher 0.5 [15]. The migration of Sc to cubic $Al_{(1-x)}Sc_xN$

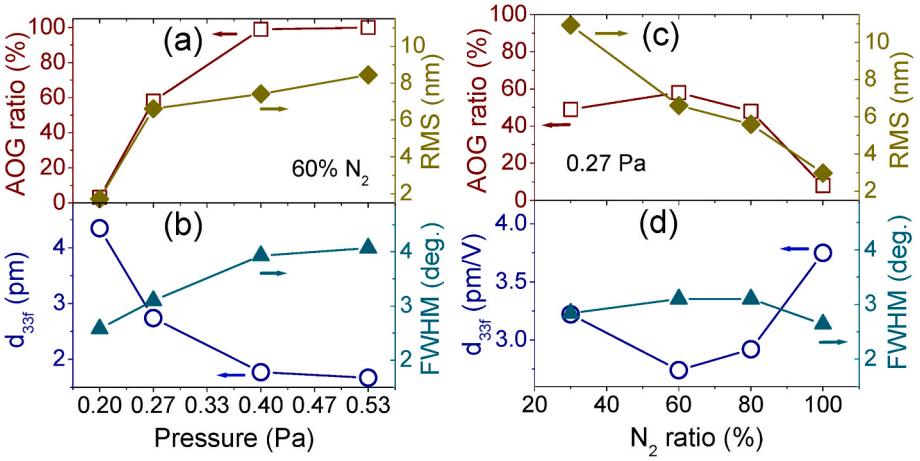

Fig. 5. Nitride film properties as a function of working pressure with 60 % N_2 gas ratio (a, b), and N_2 gas ratio at 0.27 Pa working pressure (c, d).

may lower the Sc concentration in wurtzite nitride [15], thus decreasing its *c* lattice constant, which together with the stress reduction (see Fig. 7), gives rise to the moving back to higher angle of 002 peak.

We note that from the point of view of crystal structure formation, so the piezoelectricity, or of in-plane stress development, hence the band gap the key factor is the kinetic energy of the particles arriving at the film surface, which depends on working pressure, gas ratio, and TSD [20,42]. Unfortunately, in many reports there is the lack of data on TSD and target tilt, e.g. refs. 15, 24, 26, which makes the interpretation and comparison of their results difficult.

Fig. 7 presents the residual in-plane stress and the optical band gap as a function of Sc fraction in thin nitride film deposited at 0.2 Pa with 60 % N_2 gas ratio. The stress was characterized as compressive, i.e. the measured values are negative, and its magnitude increases with increasing Sc fraction up to ca. 0.28, then decreases for further Sc fraction increase. The stress for Sc fraction of 0.41 is about 0.7 GPa compared to 0.5 and 2.1 GPa of zero and 0.27 Sc fraction, respectively. The stress increase in the first stage can be associated to the lattice distortion due to Sc atom incorporation into Al lattice sites [15,25,27]. At higher Sc fraction ($x > 0.32$), however, the softening of the crystal, together with the formation of the stable ScN may play a role in the decrease of residual stress [25,26,28].

The band gap versus Sc fraction curve has similar character to that of stress up to ca. 0.33 Sc fraction showing stress induced by Sc incorporation can be used in band gap engineering [43]. However, the gap values are significantly lower compared to that in ref. 13, probably due to high additional stress realized *via* peening effect during deposition. For *x* larger than 0.33 the gap hardly changes with increasing Sc content, and remains between 2.7 and 2.9 eV similarly to that reported in ref. 13. The reason of this behavior may be the criterion of the absorption onset ($k > 0$) together with the formation of cubic ScN phase (see Fig. 1) possessing $E_g \sim 2.5$ eV [13], which may restrain the gap from getting back to high value in spite of stress relaxation.

The averaged effective piezoelectric constants d_{33f} measured by PFM and Piezometer on bare surface of nitride film and with top electrodes are presented on Fig. 8 as a function of Sc fraction. Using top electrode, the measured values are higher. The d_{33f} increase with increasing Sc fraction, gets its highest value for Sc fraction around 0.41, then falls to almost zero at $x \sim 0.5$.

The trend of d_{33f} change with Sc content is similar to that report in literature [25,44], but our corresponding values are lower. The increase of d_{33f} with Sc content can be explained by the distortion of the wurtzite structure and the softening of the chemical bonding by alloying with Sc [25,28]. The drop of d_{33f} at high Sc content may be the consequence of the formation of dominating cubic phase $Al_{(1-x)}Sc_xN$ at such atomic composition [11,15].

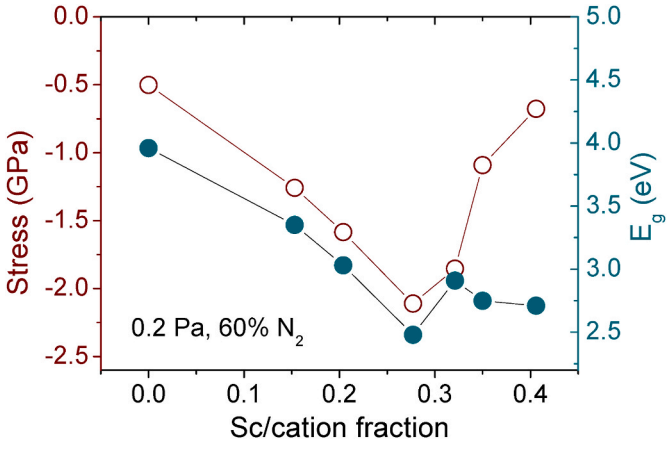

Fig. 7. In-plane residual stress, and optical band gap as a function of Sc/cation ratio for films deposited at 0.2 Pa with 60 % N_2 gas ratio.

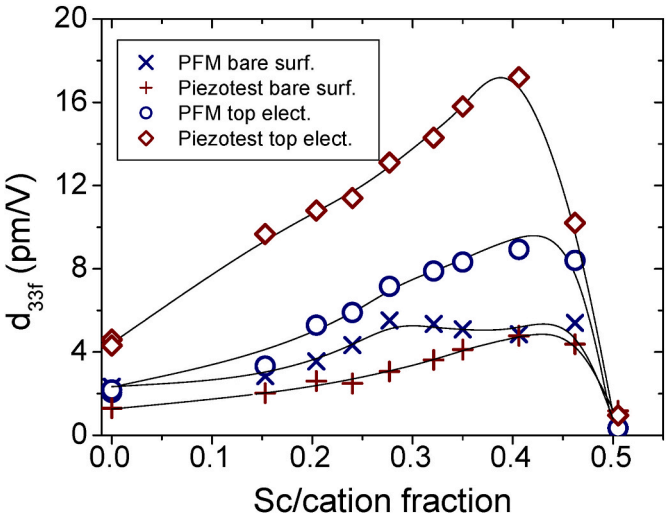

Fig. 8. Effective piezoelectric coefficient d_{33f} measured by PFM and Piezometer on bare surface and with top electrode as a function of Sc fractions. Lines are to guide the eyes. For the unit of Y axis note that 1 m/V = 1 C/N.

For direct piezoelectric measurement surface contamination can locally prevent the charge transfer between the top of nitride layer and the measuring head leading to lower d_{33} value. In contrast, top electrode conserves the pristine cleaned surface from ambient, and help to collect the generated charge from surface of nitride layer. In the case of converse piezoelectric measurement (PFM) of thin film deposited on non-piezoelectric substrate the restraining effect of the unexcited volume around the sharp PFM tip gives rise to small d_{33f} measured on the bare film. It can be eliminated by using top electrode large enough that results in higher d_{33f}. However, too large top electrode, i.e. the excited volume leads to sample bending, thus to much more surface displacement compared to the pure out plan EM displacement [37]. Also, it may result in large *AC* current through the PFM tip during the measurement with V_{ac}, which can destroy the conductive coating of the tip at its apex. Our estimation using simple simulation by finite element method shows that top electrode with lateral dimension at least two times larger than the film thickness can fulfill the requirement above, i.e. it ensures homogeneous electric field underneath, and the restraining effect is negligible (Fig. S5 in SI). This is the case of our 2 μm diameter top electrode applied on nitride film with thickness in the range from 400 to 600 nm.

The results above suggest that the nitride film deposited under low working pressure, medium N_2 gas ratio with high Sc fraction (0.2 Pa, 60 %, and 0.41, respectively) in long TSD (~ 15 cm) sputtering system may be the optimal case among the samples. It shows the highest effective piezoelectric constant, relatively low residual stress, and still smooth surface with RMS of 1 nm, and AOG areal ratio of 1 %.

3.3. Quantitative determination of piezoelectric constant by PFM

As shown on Fig. 8, the d_{33f} measured by PFM on top electrode are much lower than the corresponding values reported in literature [25,44]. To obtain more correct result (d_{33corr}), the clamping effect of substrate is also to be taken into accounts [38], which are in the following forms for converse (*cp*) and direct (*dp*) piezoelectric measurement

$$d_{33corr\_cp} = \frac{d_{33f\_cp}(s_{11}+s_{12})}{(s_{11}+s_{12}+s_{13})} \quad (1)$$

$$d_{33corr\_dp} = \frac{d_{33f\_dp}(s_{11}+s_{12})}{\left(s_{11}+s_{12}+s_{13}+\sigma/_{Y}\right)} \quad (2)$$

where σ and Y are the Poisson's ratio and the Young's modulus of the

substrate, respectively, and $s_{13} \sim 0.5\, s_{33}$ is assumed.

We used the values of the elastic constant C_{ij} calculated by Caro et al. using density functional theory (DFT) [45] for substrate effect correction of the d_{33f} measured with top electrode. The elastic compliance constants s_{ij} can be calculated by inversion of the C_{ij} matrix. Fig. 9 shows the so corrected piezoelectric coefficients determined by converse and direct piezoelectric measurements using top electrode for films deposited at 0.2 Pa with 60 % N_2 gas ratio. The corrected d_{33corr} values are in good agreement with each other, in the range of Sc fraction up to ca. 0.35. At higher Sc concentration their difference becomes significant. This may come from the fact that pure wurtzite crystal cell was applied for DFT calculation, while there are many factors affecting the piezoelectric and elastic properties of the deposited $Al_{(1-x)}Sc_xN$ films, such as crystal softening [25,27,28], formation of multi-phase [11,15] and Sc migration [15,41]. The impact of these phenomena is particularly strong for Sc fraction beyond 0.35 leading to big difference between PFM and Piezometer. Therefore, we can conclude that quantified PFM using top electrode and clamping correction is applicable for thin $Al_{(1-x)}Sc_xN$ film with x up to around 0.35.

The samples used in Fig. 9 are relatively homogeneous, i.e. the AOG areal ratio is almost negligible. For inhomogeneous sample, the corrected d_{33corr} is lower being an average. Using top electrode for "on site" calibration, one could obtain the distribution of d_{33corr} from d_{33f} measured by PFM on bare film as

$$d_{33corr} = \frac{d_{33fta}}{d_{33fba}} \times \frac{(s_{11}+s_{12})}{(s_{11}+s_{12}+s_{13})} \times d_{33fb} \qquad (3)$$

where d_{33fta} is the averaged effective piezoelectric coefficient measured with top electrode, d_{33fba} and d_{33fb} are the average and individual values measured on bare nitride, respectively. The first component is the matrix effect correction, and the second one is the substrate clamp effect correction. Fig. 10 shows d_{33corr} images in nano scale for samples having Sc fraction of about 0.24, but deposited under different conditions, specifically 0.2 Pa, 60 % N_2 and 0.27 Pa, 30 % N_2. While the surface in former case is smooth, and the d_{33corr} value is almost constant around 11 pmV^{-1}, the later case shows long grains on layer surface, but their d_{33corr} are strongly varies between zero and 11 pmV^{-1}, meaning they growth in different orientation.

4. Summary and conclusion

The influence of deposition parameters on the properties of $Al_{(1-x)}Sc_xN$ films prepared using pulse DC magnetron co-sputtering with long target-to-substrate distance was investigated by Scanning Probe Microscopy (SPM), X ray Diffractometry (XRD), and DEKTAK-XT profilometer among others. We have found that the working pressure is the most critical parameter, and a pressure of 0.2 Pa or less is needed to produce nitride film with good piezoelectricity. At higher working pressure both piezoelectricity and layer surface deteriorate due to the crystal growth in the other preferential direction, than c-axis. The impact of N_2 gas ratio on d_{33} is not so significant, however, high N_2 gas ratio can reduce the formation of AOGs. Furthermore, significant stress formed with decreasing pressure, and increasing N_2 ratio, which may be utilized for band gap tuning. The AlScN film deposited using low working pressure, medium N_2 gas ratio, and high Sc fraction, specifically 0.2 Pa, 60 %, and 0.41, respectively in our long TSD (~ 15 cm) sputtering system has high effective piezoelectric constant, relatively low residual stress, still smooth surface, and low AOG areal ratio. We have shown the beneficial use of top electrode against the matrix restraining effect for PFM measurement of piezoelectric constant of thin film. Applying proper top electrode together with substrate clamping correction, the result of PFM is in good agreement with those obtained from direct piezoelectric method (Piezometer) as far as the DFT calculated elastic compliance constants s_{ij} remain realistic, i.e. $x < 0.35$. This reveals the applicability of PFM as a quantitative method to study the piezoelectric properties of thin films under the aforementioned conditions.

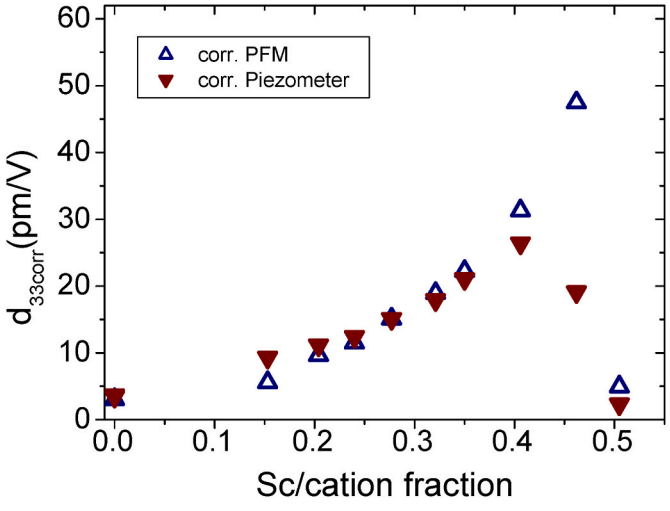

Fig. 9. Corrected d_{33corr} values of d_{33f} determined by Piezometer and PFM using top electrode as a function of Sc fraction in nitride film deposited at 0.2 Pa with 60 % N_2 gas ratio. For the unit of Y axis note that 1 m/V = 1 C/N.

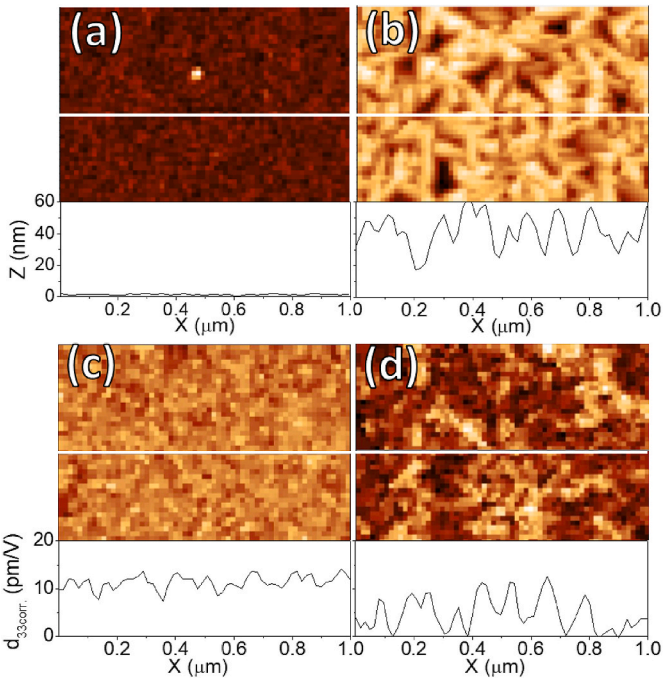

Fig. 10. *Morphology and d_{33corr} maps of nitride film having 0.24 Sc fraction deposited at 0.2* Pa*, 60 % N_2 (a,c) and 0.27* Pa*, 30 % N_2 (b, d). White lines indicate the line-cuts.*

CRediT authorship contribution statement

Nguyen Quoc Khánh: Writing – original draft, Investigation, Conceptualization. **Zsolt Endre Horváth:** Writing – review & editing, Investigation. **Zsolt Zolnai:** Writing – review & editing, Investigation. **Péter Petrik:** Investigation. **László Pósa:** Investigation. **János Volk:** Writing – review & editing, Funding acquisition, Conceptualization.

Declaration of competing interest

The authors declare that they have no known competing financial interests or personal relationships that could have appeared to influence

the work reported in this paper.

Data availability

Data will be made available on request.

Acknowledgement

This work was supported by the National Research, Development and Innovation Fund of the Hungarian Government in the framework of KoFAH, NVKP_16-1-2016-0018 and TKP2021-NVA-03. Support of Grant no. K131515 OTKA is also gratefully acknowledged. The authors thank Levente Illés for SEM and EDS measurement, and Erika Tunyogi for assistance in PFM evaluation.

Appendix A. Supplementary data

Supplementary data to this article can be found online at https://doi.org/10.1016/j.mssp.2023.107902.

References

[1] H. Bishara, S. Berger, Piezoelectric ultra-sensitive aluminum nitride thin film on flexible aluminum substrate, J. Mater. Sci. Electron. Mat. 53 (2018) 1246–1255, https://doi.org/10.1007/s10853-017-1566-8.
[2] L. Natta, V.M. Mastronardi, F. Guido, L. Algieri, S. Puce, F. Pisano, F. Rizzi, R. Pulli, A. Qualtieri, M. De Vittorio, Soft and flexible piezoelectric smart patch for vascular graft monitoring based on Aluminum Nitride thin film, Sci. Rep. 9 (2019) 8392, https://doi.org/10.1038/s41598-019-44784-1.
[3] Z. Shi, X. Lu, X. Tang, D. Wang, Z. Cong, X. Ma, Y. Hao, Stress enhanced photoelectric response in flexible AlN single-crystalline thin films, Appl. Surf. Sci. 585 (2022), 152378, https://doi.org/10.1016/j.apsusc.2021.152378.
[4] F. Narita, M. Fox, A review on piezoelectric, magnetostrictive, and magnetoelectric materials and device technologies for energy harvesting applications, Adv. Eng. Mater. (2017), 1700743, https://doi.org/10.1002/adem.201700743.
[5] X. He, Q. Wena, Zh Lua, Zh Shang, Zh Wen, A micro-electromechanical systems based vibration energy harvester with aluminum nitride piezoelectric thin film deposited by pulsed direct-current magnetron sputtering, Appl. Energy 228 (2018) 881–890, https://doi.org/10.1016/j.apenergy.2018.07.001.
[6] J. Zhao, J. Han, Y. Xing, W. Lin, L. Yu, X. Cao, Zh Wang, X. Zhou, X. Zhang, B. Zhang, Fabrication and application of flexible AlN piezoelectric film, Semicond. Sci. Technol. 35 (2020), 035009, https://doi.org/10.1088/1361-6641/ab6bb0.
[7] U.C. Kaletta, P.V. Santos, D. Wolansky, et al., Monolithic integrated SAW filter based on AlN for high-frequency applications, Semicond. Sci. Technol. 28 (6) (2013) 1–7, https://doi.org/10.1088/0268-1242/28/6/065013.
[8] F. Wang, F. Xiao, D. Song, L. Qian, Y. Feng, B. Fu, K. Dong, C. Li, K. Zhang, Research of micro area piezoelectric properties of AlN films and fabrication of high frequency SAW devices, Microelectron. Eng. 199 (2018) 63–68, https://doi.org/10.1016/j.mee.2018.07.016.
[9] V. Mortet, M. Nesladek, K. Haenen, A. Morel, M. D'Olieslaeger, M. Vanecek, Physical properties of polycrystalline aluminium nitride films deposited by magnetron sputtering, diamond relat, Materials 13 (2004) 1120, https://doi.org/10.1016/j.diamond.2003.10.082.
[10] Y.Q. Fu, J.K. Luo, N.T. Nguyen, A.J. Walton, A.J. Flewitt, X. T Zu, Y. Li, G. McHale, A. Matthews, E. Iborra, H. Dui, W.I. Milne, Advances in piezoelectric thin films for acoustic biosensors, acoustofluidics and lab-on-chip applications, Prog. Mater. Sci. 89 (2017) 31–91, 10.1016/j.pmatsci.2017.04.006 and refs therein.
[11] M. Akiyama, T. Kamohara, K. Kano, A. Teshigahara, Y. Takeuchi, N. Kawahara, Enhancement of piezoelectric response in scandium aluminum nitride alloy thin films prepared by dual reactive cosputtering, Adv. Mater. 21 (2009) 593–596, https://doi.org/10.1002/adma.200802611.
[12] P.M. Mayrhofer, H. Riedl, H. Euchner, M. Stöger-Pollach, P.H. Mayrhofer, A. Bittner, U. Schmid, Microstructure and piezoelectric response of YxAl1−xN thin films, Acta Mater. 100 (2015) 81–89, https://doi.org/10.1016/j.actamat.2015.08.019.
[13] R. Deng, S.R. Evans, D. Gall, Bandgap in $Sc_xAl_{1-x}N$, app, Phys. Lett. 102 (2013), 112103, https://doi.org/10.1063/1.4795784.
[14] S. Fichtner, N. Wolff, F. Lofink, L. Kienle, B. Wagner, AlScN: a III-V semiconductor based ferroelectric, J. Appl. Phys. 125 (2019), 114103, https://doi.org/10.1063/1.5084945.
[15] S. Satoh, K. Ohtaka, T. Shimatsu, Sh Tanaka, Crystal structure deformation and phase transition of AlScN thin films in whole Sc concentration range, J. Appl. Phys. 132 (2022), 025103, https://doi.org/10.1063/5.0087505.
[16] G.L. Huffman, D.E. Fahnline, R. Messier, L.J. Pilione, Stress dependence of reactively sputtered aluminum nitride thin films on sputtering parameters, J. Vac. Sci. Technol. A Vac. Surfaces, Film 7 (1989) 2252–2255, https://doi.org/10.1116/1.575923.
[17] M. Ishihara, S.J. Li, H. Yumoto, K. Akashi, Y. Ide, Control of preferential orientation of AlN films prepared by the reactive sputtering method, Thin Solid Films 316 (1998) 152, https://doi.org/10.1016/S0040-6090(98)00406-4.
[18] X. Xu, H. Wu, C. Zhang, Z. Jin, Morphological properties of AlN piezoelectric thin films deposited by DC reactive magnetron sputtering, Thin Solid Films 388 (2001) 62, https://doi.org/10.1016/S0040-6090(00)01914-3.
[19] M. Reusch, K. Holc, W. Pletschen, L. Kirste, A. Žukauskaitė, T. Yoshikawa, D. Iankov, O. Ambacher, V. Lebedev, Analysis and optimization of sputter deposited AlN-layers for flexural plate wave devices, J. Vac. Sci. Technol. B 34 (2016), 052001, https://doi.org/10.1116/1.4959580.
[20] Y. Lu, M. Reusch, N. Kurz, A. Ding, T. Christoph, L. Kirste, V. Lebedev, A. Žukauskaitė, Surface morphology and microstructure of pulsed DC magnetron sputtered piezoelectric AlN and AlScN thin films, Phys. Status Solidi A 215 (2018), 1700559, https://doi.org/10.1002/pssa.201700559.
[21] R. Supruangnet, W. Sailuam, W. Busayaporn, Ch Wattanawikkam, A. Jiamprasertboon, A. Ruangvittayanon, W. Sangsai, A. Pirasampansiri, S. Limpijumnong, R. Yimnirun, A. Bootchanont, Effects of N2-content on formation behavior in AlN thin films studied by NEXAFS: theory and experiment, J. Alloys Compd. 844 (2020), 156128, https://doi.org/10.1016/j.jallcom.2020.156128.
[22] D.W. Hoffman, J.A. Thornton, The compressive stress transition in Al, V, Zr, Nb and W metal films sputtered at low working pressures, Thin Solid Films 45 (1977) 387–396, https://doi.org/10.1016/0040-6090(77)90276-0.
[23] G. Ross, H. Dong, C.B. Karuthedath, A.T. Sebastian, T. Pensala, M. Paulasto-Kröckel, The impact of residual stress on resonating piezoelectric devices, Mater. Des. 196 (2020), 109126, https://doi.org/10.1016/j.matdes.2020.109126.
[24] S. Fichtner, T. Reimer, S. Chemnitz, F. Lofink, B. Wagner, Stress controlled pulsed direct current cosputtered $Sc_xAl_{1-x}N$ as piezoelectric phase for micromechanical sensor applications, Apl. Mater. 3 (2015), 116102, https://doi.org/10.1063/1.4934756.
[25] O. Zywitzki, T. Modes, S. Barth, H. Bartzsch, P. Frach, Effect of scandium content on structure and piezoelectric properties of AlScN films deposited by reactive pulse magnetron sputtering, Surf. Coating. Technol. 309 (2017) 417–422, https://doi.org/10.1016/j.surfcoat.2016.11.083.
[26] D. Solonenko, Ch Lan, C. Schmidt, C. Stoeckel, K. Hiller, D.R.T. Zahn, Co-sputtering of Al(1-x)Sc(x)N thin films on Pt(111): a characterization by Raman and IR spectroscopies, J. Mater. Sci. Mater. Electron. 55 (2020) 17061–17071, https://doi.org/10.1007/s10853-020-05244-8.
[27] F. Tasnádi, B. Alling, C. Höglund, G. Wingqvist, J. Birch, L. Hultman, I. A. Abrikosov, Origin of the anomalous piezoelectric response in wurtzite $Sc_xAl_{1-x}N$ alloys, Phys. Rev. Lett. 104 (2010), 137601, https://doi.org/10.1103/PhysRevLett.104.137601.
[28] R. Deng, K. Jiang, D. Gal, Optical phonon modes in $Sc_xAl_{1-x}N$, J. Appl. Phys. 115 (2014), 013506, https://doi.org/10.1063/1.4861034.
[29] M. Stewart, M.G. Cain, Direct Piezoelectric Measurement: the Berlincourt Method, Springer Series in Measurement Science and Technology, 2014, pp. 37–64, https://doi.org/10.1007/978-1-4020-9311-1_3.
[30] E. Soergel, Piezoresponse force microscopy (PFM), J. Phys. D Appl. Phys. 44 (2011), 464003, https://doi.org/10.1088/0022-3727/44/46/464003.
[31] S. Jesse, S. Guo, A. Kumar, B.J. Rodriguez, R. Proksch, S.V. Kalinin, Nanotechnology 21 (2010), 405703, https://doi.org/10.1088/0957-4484/21/40/405703.
[32] A. Gruverman, M. Alexe, D. Meier, Nat. Commun. 10 (2019) 1661, https://doi.org/10.1038/s41467-019-09650-8.
[33] A. Abdollahi, N. Domingo, I. Arias, G. Catalan, Converse flexoelectricity yields large piezoresponse force microscopy signals in non-piezoelectric materials, Nat. Commun. 10 (2019) 1266, https://doi.org/10.1038/s41467-019-09266-y.
[34] D. Seol, S. Park, O.V. Varenyk, S. Lee, H.N. Lee, A.N. Morozovska, Y. Kim, Determination of ferroelectric contributions to electromechanical response by frequency dependent piezoresponse force microscopy, Sci. Rep. 6 (2016), 30579, https://doi.org/10.1038/srep30579.
[35] N.Q. Khánh, J. Radó, Zs E. Horváth, S. Soleimani, B. Oyunbolor, J. Volk, The effect of substrate bias on the piezoelectric properties of pulse DC magnetron sputtered AlN thin films, J. Mater. Sci. Mater. Electron. 31 (2020) 22833–22843, https://doi.org/10.1007/s10854-020-04810-9.
[36] S. Kim, D. Seol, X. Lu, M. Alexe, Y. Kim, Electrostatic-free piezoresponse force microscopy, Sci. Rep. 7 (2017), 41657, https://doi.org/10.1038/srep41657.
[37] L. Jaloustre, S. Le Denmat, T. Auzelle, M. Azadmand, L. Geelhaar, F. Dahlem, R. Songmuang, Toward quantitative measurements of piezoelectricity in III-N semiconductor nanowires, ACS Appl. Nano Mater. 4 (2021) 43–52, https://doi.org/10.1021/acsanm.0c02078.
[38] K. Lefki, G.J.M. Dormans, Measurement of piezoelectric coefficients of ferroelectric thin films, J. Appl. Phys. 76 (1994) 1764, https://doi.org/10.1063/1.357693.
[39] D. Nečas, P. Klapetek, Gwyddion: an open-source software for SPM data analysis, Cent. Eur. J. Phys. 10 (2012) 181, https://doi.org/10.2478/s11534-011-0096-2.
[40] R.A. Jaccodine, W.A. Schlegel, Measurement of strains at Si-SiO2 InterfaceJ, Appl. Phys. 37 (1966) 2429–2434, https://doi.org/10.1063/1.1708831.
[41] C. Silviu Sandu, F. Parsapour, S. Mertin, V. Pashchenko, R. Matloub, T. LaGrange, B. Heinz, P. Muralt, Abnormal grain growth in AlScN thin films induced by complexion formation at crystallite interfaces, Phys. Status Solidi A 216 (2019), 1800569, https://doi.org/10.1002/pssa.201800569.
[42] S. Fichtner, N. Wolff, G. Krishnamurthy, A. Petraru, S. Bohse, F. Lofink, S. Chemnitz, H. Kohlstedt, L. Kienle, B. Wagner, Identifying and overcoming the interface originating c-axis instability in highly Sc enhanced AlN for piezoelectric micro-electromechanical systems, J. Appl. Phys. 122 (2017), 035301, https://doi.org/10.1063/1.4993908.

[43] Y. Sun, S.E. Thompson, T. Nishida, Physics of strain effects in semiconductors and metal-oxide-semiconductor field-effect transistors, J. Appl. Phys. 101 (2007), 104503, https://doi.org/10.1063/1.2730561.
[44] M. Akiyama, K. Kano, A. Teshigahara, Influence of growth temperature and scandium concentration on piezoelectric response of scandium aluminum nitride alloy thin films, Appl. Phys. Lett. 95 (2009), 162107, https://doi.org/10.1063/1.3251072.
[45] M.A. Caro, S. Zhang, T. Riekkinen, M. Ylilammi, M.A. Moram, O. Lopez-Acevedo, J. Molarius, T. Laurila, Piezoelectric coefficients and spontaneous polarization of ScAlN, J. Phys. Condens. Matter 27 (2015), 245901, https://doi.org/10.1088/0953-8984/27/24/245901.